Available online at www.sciencedirect.com

ScienceDirect

Procedia CIRP 95 (2020) 915–920

www.elsevier.com/locate/procedia

20th CIRP Conference on Electro Physical and Chemical Machining (ISEM 2020)

Surface micro and nanostructuring of three-dimensional components of micro medical devices

Francesco Biondani[a]*, Lorenzo Benassi[b], Giuliano Bissacco[a], Leonardo Orazi[b], Peter T. Tang[c] *

[a]*Technical University of Denmark, Department of Mechanical engineering, Produktionstorvet, Kgs. Lyngby 2800, Denmark*
[b]*University of Modena and Reggio Emilia, DISMI, via Amendola 2, Reggio Emilia 41122, Italy*
[c]*IPU, Diplomvej 376, Kgs. Lyngby 2800, Denmark*

* Corresponding author. Tel.: +45 45254733; E-mail address: frgbio@mek.dtu.dk

Abstract

Surface structuring of medical implants has been shown to reduce the rejection rate of medical devices inserted inside living tissue. Several studies have shown that by texturing the surface of medical implants at micro/nanoscale it is possible to foster cell adhesion. The surface texturing of medical devices poses many challenges in terms of cost and time when the nano texturing process is performed directly on the part surface. A viable solution for mass production of polymer based surface enhanced medical devices is achieved via injection molding. However, nano structuring of micro injection molding molds, requires techniques enabling processing of complex surfaces, small curvature radii and with high aspect ratios. Furthermore the accessibility of all surfaces to be structured and the processing time are the main concerns and limiting factors on the selection of the structures dimensions and geometries. In this work, two different process chains are analyzed for the nano structuring of a bone micro plug. The first method relies on a chemical deposition process in order to produce a semi random structure on the entire mold surface of the medical component. The characteristic size of the structures is controlled by acting on the deposition parameters. The second process, relies on laser structuring of the mold components by producing Laser-Induced Periodic Surface Structures (LIPSS).The two process chains are compared and an evaluation of the applicability in different production scenarios presented, with specific focus on surface accessibility, nano structures uniformity and applicability to surfaces with complex geometry

Keywords: Nanostructuring; Medical devices; free form surfaces;

1. Introduction

Medical implants are devices inserted inside the human body in order to replace, repair or enhance specific biological tissues. When a medical implant is directly implanted into bone tissue, its ability to bond with the surrounding matrix is known as osseointegration. Many medical implants for dental, orthopedic and maxillofacial surgery relay on osseointegration.

A correct osseointegration is crucial for the implant performance: it leads to better stability of the implanted device, it promotes the healing process and allows faster loading of the implant [1].

In order to promote osseointegration, an ideal medical implant should have mechanical properties comparable with those of the surrounding tissue and should not provoke any inflammatory reaction.

Many research efforts have been devoted towards the improvement of the bone/implant osseointegration, with the aim of fostering healing and adherence of the implant to the surrounding material.

Enhanced device osseointegration can be achieved by designing materials that act as scaffold for the cells and promote cells interconnections [2].

Already 40 years ago, the surface structure was recognized to be one of the important factors for implants integration into the bones [3].

A review by [4] showed a direct correlation between surface texture, bone-implant integration and push out strength. The surface structure of a medical implant elicits cell adhesion

10.1016/j.procir.2020.01.178

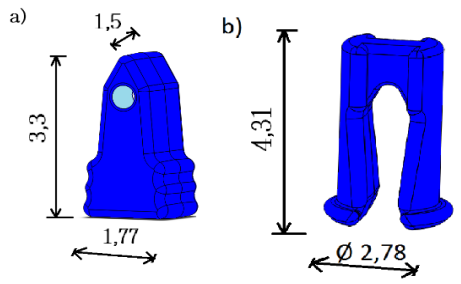

Fig. 1. (a) plug component; (b) anchor component. Dimensions in mm.

on a multidimensional scale [5]. At the microscale, a rough surface presents a higher contact area, thus increases biomechanical interlocking with the bone. At the nanoscale, the surface texture increases the surface energy, promoting bone cell migration, spreading and proliferation.

However, the selection of the optimal surface texture for a medical implant is still object of debate. It is commonly agreed that the optimal structure is strictly related to the nature of the host tissue surrounding the implant itself. A great deal of publications have described the in-vitro and in-vivo behavior of substrates textured with micro pillars [6], microgrooves [7] and porous structures [8]. In recent years, an increased recognition toward the roles of surface nano features in cell proliferation has led to extensive studies on nano textured implants [9],[10].

Beside selection of the optimal surface texture, the availability of suitable manufacturing process chains for the production of such texture on medical implants is another crucial point.

The manufacturing process for a textured medical device needs to be reliable, cost effective and independent from the underlying macro geometry of the components. While many surface texturing processes are suitable for planar surfaces, few are able to deal with the complexity of free form components and even less can cope with mass production requirements [11].

In this work, two different process chains for surface nanostructuring of 3D medical micro components are described and analyzed. The first one consists in a chemical deposition process that generates a randomly oriented nanostructure. The second one, based on laser texturing is able to originate nano features with controllable orientation. Both these processes are used for nanostructuring mold components for mass production of a medical micro implant in polymer by micro injection molding.

2. Test case

The presented work focuses on the nanotexturing of an implant for ligaments reattachment shown in figure 1.

The device consists in two parts: a pin part here referred as *plug* (figure 1a), and a flexible component, here referred as *anchor* (figure 1b). The operative procedure for the insertion of the implant can be divided in five steps: i) a hole is drilled into the bone, ii) a suture wire is inserted in the plug hole, iii) the plug is inserted into the bone, iv) the anchor is inserted into the bone, v) the suture is pulled to lock the plug into the anchor. Once the device is in place and the tendon secured with the suture wire, any further tension on the implant will cause the plug to further penetrate into the anchor. The penetration of the plug will expand the anchor thereby increasing the interference fit of the implant with the bone material.

Both anchor and plug are produced using micro injection molding. To obtain a nano texture on the polymer parts, the opposite texture geometry is generated on the mold cavities and the texture is then replicated on the polymer parts during injection molding.

3. Nanostructuring techniques

The complex geometry of the micro implant poses several accessibility limitations for the surface texturing techniques.

The mold for the components in figure 1 is characterized by features with high aspect ratio and nearly 90^0 side walls that are hardly affected by line-of-sight texturing processes.

In this work two different techniques for surface nano structuring are compared: a chemical deposition process and a laser texturing process.

Chemical processes, being relatively independent from the component geometry, are good candidates for effective 3D nano texturing, therefore electrolytic deposition of copper was chosen for the purpose. Copper electroplating relies on the dissolution of a copper source (anode) inside an electrolytic cell. The dissolved copper ions travel inside the electrolytic bath and deposit over the surface of the mold insert (cathode). The result is a thin coating of pure copper with tailored surface topography depending on deposition parameters and bath composition [12].

LIPSS, or Laser-induced Periodic Surface Structures, are oriented nanostructures resulting from a specific laser texturing process. They consist in periodic ripples generated over the surface after laser irradiation of polarized ultrashort pulses with intensities above the material's ablation threshold. Orientations and pitch of the LIPSS can be controlled by acting on the polarization plane, on the incidence angle, on the laser wavelength and on the pulse fluence [10].

4. Experimental procedure

For the feasibility study of the proposed nano structuring methods, two inserts were micro machined in two different materials. The first mold insert was produced using CW008A oxygen-free copper. Although copper molds are not as durable as, for example, steel molds, copper ensures good bonding properties with the electrodeposited coating. Furthermore, the extremely high heat conductivity of copper ensures a low cycle time for the injection molding process. The second mold insert was machined in IMPAX, a commonly used tool steel material with hardness in the range of 30-40 HRC. A schematic drawing of one of the molds inserts is shown in figure 2.

4.1. Electroplating procedure

Copper electroplating was performed over the copper insert surface. Prior to deposition, the insert was thoroughly cleaned by means of cathodic degreasing and the naturally formed oxide layer was removed in a dry acid solution. The plating procedure was performed in an electrolyte solution described

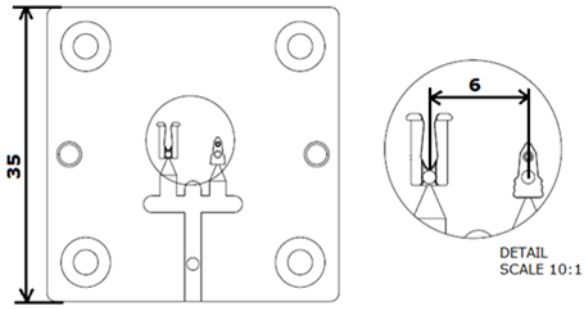

Fig. 2. Schematic drawing of one of the mold inserts.

in [12] at room temperature. Agitation of the electrolyte solution was achieved by means of a controlled stream of air.

In order to achieve a nanostructured surface a steady DC current of 16 A/dm^2 was applied to the electrolytic cell.

The copper plating bath was originally made for pulse reverse plating [12] and contains no organic additives to promote a smooth deposit. By applying the relatively high DC current density of 16 A/dm², the growth of an increasingly rough deposit is sustained for as long as the current is on. The process was carried out for a total 1.40 minutes. It is important not to exceed the set deposition time, as this will lead to dimensional changes due to the increased coating thickness.

In order to evaluate the effect of the coating process on the surface roughness and overall dimensions of the component, preliminary electrodeposition tests were carried out on polished copper samples on which a microgroove was machined. Some flat areas of the samples were partially masked to avoid deposition. The coating thickness was evaluated after deposition on the partially masked surfaces and through the dimensional change of the micro grooves.

4.2. Laser texturing procedure

LIPSS were generated on the steel insert using a C.B Ferrari LS 1300 3-axis laser machine, equipped with Hyper Rapid Picosecond Laser produced by Coherent laser. The laser processing parameters, listed in table 1, were selected after initial tuning on a flat block of IMPAX steel. A unique laser focal plane, positioned at the average depth of the insert cavity, was selected for structuring the entire cavity. While this choice is not ideal, it allows to cope with the lack of additional rotational axis of the machine tool and avoid manual repositioning of the insert. Given the selected overlapping of the laser path, the laser spot size and fluence per pulse, the machined area is exposed to an average fluence of 23 J/cm^2.

Table 1. Laser scanning parameters used for generating the LIPSS

Scanning parameters	
Scan velocity	2500 mm/s
Hatch distance	10 µm
Frequency	1 MHz
Pulse duration	10 ps
Spot size/ Focal length	25 µm at spot size/ 160 mm
Wavelength	1064 nm
Beam quality	M^2<1.3
Fluence per pulse	0.89 J/cm^2
Peak fluence per pulse	89 GW/cm^2

4.3. Injection molding tests

Preliminary molding experiments were carried out using ALLROUNDER 370 A, an injection molding machine produced by Arburg. Polyactic acid (PLA) and polypropylene (PP) were used in the experiments. PLA was selected because of its known bio absorbability properties (in 12 to 36 months), eliminating the need for the patients to undergo to and additional surgery for the removal of the implant. PP was taken into consideration for its known good replication properties for nanostructures.

4.4. Surface analysis

The surface of the inserts, as well as the produced plastic components were analysed by means of a Quanta FEG 200 ESEM and a confocal microscope Olympus LEXT OLS4100.

Due to accessibility issues, measurement of the LIPSS inside the mold cavity of the anchor were taken by means of the replica techniques as described in [13]. The mold cavity was filled with silicone and pressure was applied by means of a hot embossing machine for the time needed for the silicone rubber to set.

Fig. 3. Observed areas on the corresponding mold cavities. Area 1 is located on the rounding of the anchor leg, area 2 on the deepest point of the anchor cavity. Area 3 is located on the vertical wall of the plug (87.5^0) while are 4 is on a flat region of the plug cavity.

5. Experiment results

The main focus of the investigations was the assessment of the successful occurrence of the nano texturing processes. For the process chain based on electroplating, particular attention was given to the deeper cavities of the electroplated insert, where the accessibility of the electrolyte may be problematic. For the laser texturing process chain, focus is given to the quasi-vertical walls and features not coplanar with the focus plane of the laser beam. In figure 3 the observed areas are shown.

5.1. Electroplated insert analysis

Plating tests on a reference polished surface have shown that the chemical deposition process leads to an increase of surface roughness from Sa 5 nm to 125 nm, furthermore, the added

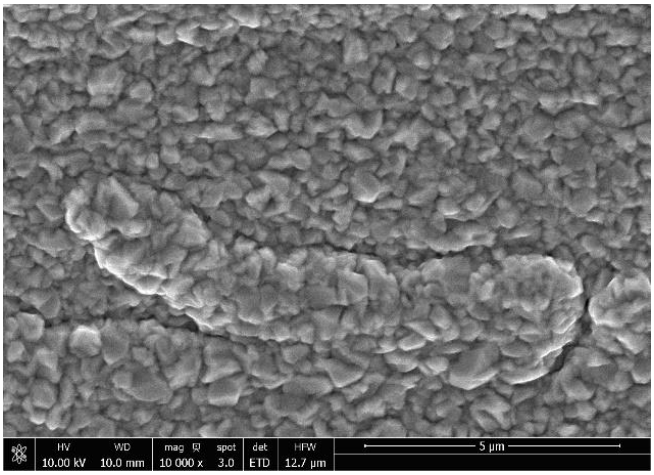

Fig. 4. Area 1 of figure 3 textured by means of electroplating.

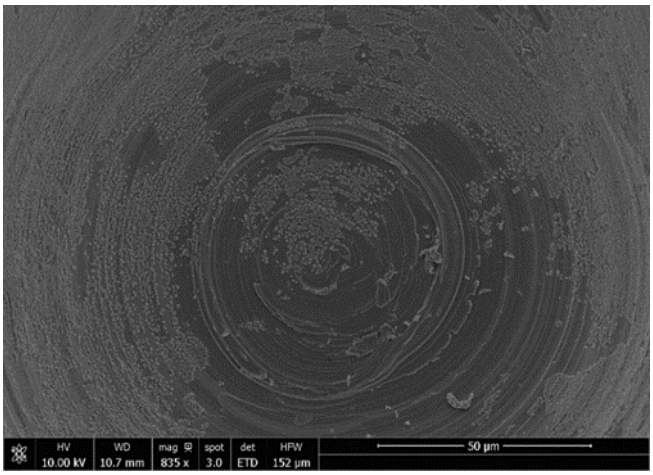

Fig. 5. Lack of texturing in Area 2 of figure3 after electroplating.

material offsets the original surface of approximately 6 µm on average for the tested process parameters.

The nanotexture surface of the mold insert after copper plating in area 1 is shown in figure 4. In this area, the copper coating has uniformly covered the surface of the mold cavity. The coating shows a non directional homogenous structure, consisting of protruding features with characteristic lateral dimension of 400-500 nm in average, as measured from SEM images.

Figure 5 shows an SEM picture of area 2: the deepest area of the anchor mold. Incomplete coverage of the surface by the copper coating is evident. The reasons for this lack nano texturing are unclear. Incomplete oxide layer removal or insufficient cleaning of the surface may be responsible. This suggests that a proper and well defined procedure for the removal of the oxide layer and thorough cleaning are of crucial importance, especially when working with micro components, where accessibility of some areas can be problematic.

5.2. Laser textured insert

The laser treated surfaces of the mold insert are shown in fig 6 and fig 7, respectively for area 1 and area 3.

Figure 6 shows well developed and well-defined LIPSS, even though the surface was not coplanar with the focus plane of the laser beam due to the radius of curvature of the part geometry in this location.

Figure 7, instead, shows the surface in area 2. As expected, the texturing of this surface is more problematic. The LIPSS show a different behaviour: the features are organized in horizontal micro bands with a 2 µm distance. This is probably due to a favourable surface orientation generated by the residual surface scallops of the pre-existing topography generated during milling (figure. 8). Whenever the relative orientation of the local surface plane and the laser focal plane is favourable, surface texturing becomes possible.

Figure 9 shows the surface on area 4, coplanar with the laser plane. Here, a well-developed surface texture is evident and comparable with the surface in figure 6. To be noticed that this latter area was not in the focal plane of the laser but it lied on a parallel plane with offset 320 µm. Changes with respect to the relative distance with the laser focal plane, even if small compared to the focal length, may cause changes in the LIPPS morphology. The pitch of the LIPSS was measured from the SEM images for area 1 and area 4 and the results are reported in table 2. The surface coplanar with the laser focal plane shows LIPSS with longer pitch.

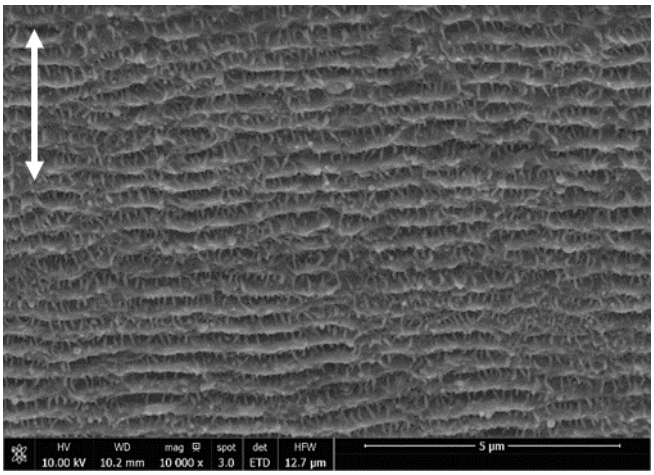

Fig. 6 LIPSS on anchor cavity, area 1 of figure 3. Laser polarization direction indicated by the arrow.

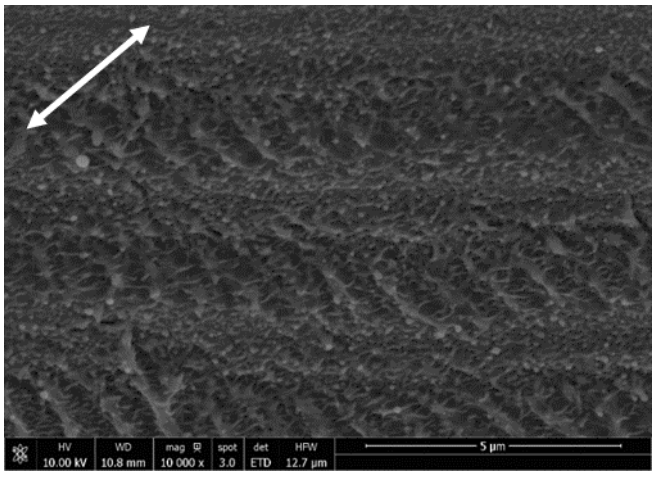

Fig. 7. LIPSS on area 3. The local surface is almost perpendicular to the laser focal plane. Laser polarization direction indicated by the arrow.

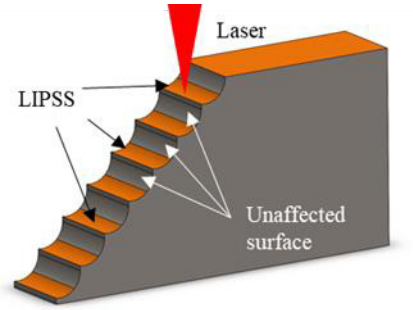

Fig. 8. The surface scallops resulting from the milling process create areas with favorable orientations (orange area) that interact with the laser beam creating LIPSS. The other parts of the surface (grey) do not interact with the laser.

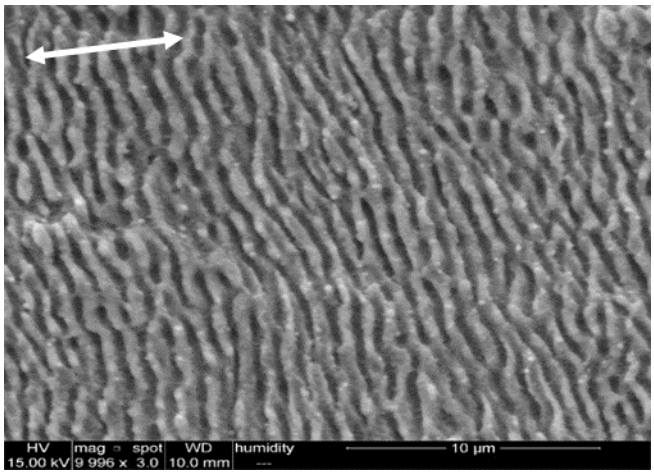

Fig. 9. LIPSS of area 4, coplanar with the laser focal plane. Laser polarization direction indicated by the arrow.

5.3. Replica analysis on LIPSS

The coverage of the mold surface by the LIPSS was analyzed by means of confocal microscopy analysis on the silicone replica of the anchor cavity. The replica allows to expose the surface of the side walls of the mold, otherwise inaccessible for confocal microscopy analysis. In figure 10 the surface roughness Sa on several areas of one of the anchor legs is shown as a function of the inclination angle between the laser focal plane and the part local surface. In order to isolate the roughness contribution of the LIPSS from other surface roughness contributions, the acquired surface images were filtered with a low pass Gaussian filter at 1 µm. This filter allows to isolate the LIPSS with a spatial wavelength in the order of 0.5 µm (detected from SEM images), while removing the effect of the milling marks with spatial wavelength in the order of 2 µm.

Figure 10 shows that, when the mold surface and the laser focal plane are aligned, the effect of the LIPSS on the surface roughness is more relevant. With the increase of the relative inclination the fraction of the local surface covered by the LIPSS and the height of the LIPSS are reduced, therefore their effect on the nano scale texture fades translating into lower Sa value.

Table 2. Mean pitch of the LIPSS

Area	Mean pitch [nm]	St. Dev. [nm]
Area 1 (figure 6)	200	38
Area 4 (figure 9)	573	95

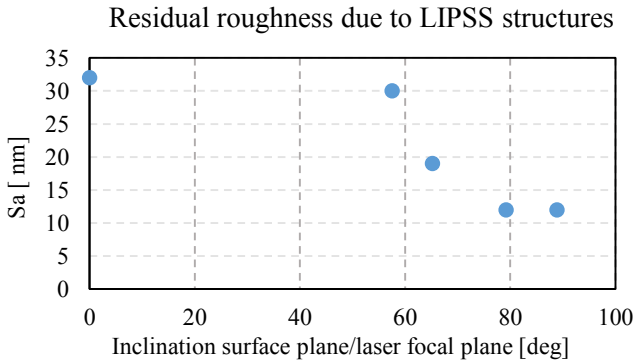

Fig. 10. Residual Sa roughness on the machine surface in relation with the relative inclination of the local plane and the laser focal plane.

6. Injection Molding tests

Two different polymers where used for preliminary injection molding trials: PP and PLA.

The injection molding parameters for both polymers are listed in table 3. It can be noticed that, due to higher viscosity of PLA, much higher injection pressure is needed in order to properly fill the cavity of the mold.

6.1. SEM replication analysis

Figures 11 and 12 show the surface of the component produced in PLA and PP respectively. The replication of the LIPSS on PP was more successful due to the lower polymer viscosity.

Regarding the parts produced by means of the copper insert no clearly distinguishable replication occurred, especially with PLA, with the selected process parameters.

7. Discussion and conclusion

In this work, two different nano structuring techniques were described and used to texture the surface of a complex 3D mold for a medical device for ligaments reattachment. Both processes have benefits and drawbacks.

The first process relies on electrochemical deposition of copper on the mold insert surface. It is a relatively fast process that does not require costly equipment. A good coverage of the surface can be achieved, even though some areas need extra caution in order to assure a proper coating deposition. The surface nano texture shows homogeneous features covering the majority of the cavities with characteristic size in the order of 400-500 nm. The added surface offset due to the coating thickness was limited to 6 µm that could be neglected for the described application. On the other hand 6 µm can be problematic for matching surfaces on the mold plates because flashing of the injected polymer may occur. Furthermore, copper is a soft material for mold manufacturing and it cannot

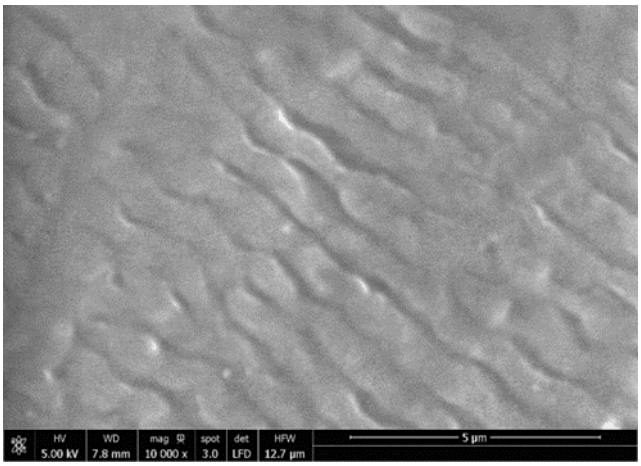

Fig. 11. Replication of LIPSS on one of the molded components in PLA

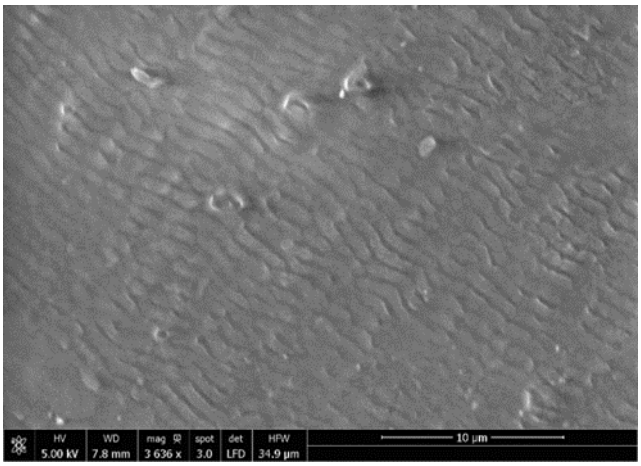

Fig. 12. Replication of LIPSS on one of the molded components in PP

compete with the service life of a steel mold in terms of molded parts. The preliminary molding trials were not successful and the surface nano textures were not reproduced on the polymer part. However, this does not exclude that with further molding parameters optimization the structures could be replicated.

The second process is a laser-based texturing method that produces a series of ripples on the surface of the component.

The process is able to texture the surface of hard materials such as tool steel, which guarantees acceptable service life in molding applications. Furthermore, a certain degree of control on the texture orientation can be achieved. The process showed difficulties in structuring geometries with surfaces with suboptimal orientation compared to the laser focal plane therefore 5 axis laser machine tools are recommended for structuring complex 3D components.

Table 3. Parameters used for injection molding

Process parameters	PLA	PP
Injection pressure [bar]	320	240
Holding pressure [bar]	220	220
Melt temperature [°C]	205	230
Mold Temperature [°C]	45	60

The preliminary injection molding study showed partial replication of the structures both on PLA and PP even though better results are achieved with the less viscous PP polymer.

Acknowledgements

CB Ferrari s.r.l. is acknowledged for the texturing of the steel inserts.

References

[1] H. S. Alghamdi, “Methods to improve osseointegration of dental implants in low quality (type-IV) bone: An overview,” *J. Funct. Biomater.*, vol. 9, no. 1, 2018.

[2] V. Rai, M. F. Dilisio, N. E. Dietz, and D. K. Agrawal, “Recent strategies in cartilage repair: A systemic review of the scaffold development and tissue engineering,” *J. Biomed. Mater. Res. - Part A*, vol. 105, no. 8, pp. 2343–2354, 2017.

[3] T. Albrektsson, P.-I. Brånemark, H.-A. Hansson, and J. Lindström, “Osseointegrated Titanium Implants: Requirements for Ensuring a Long-Lasting, Direct Bone-to-Implant Anchorage in Man,” *Acta Orthop. Scand.*, vol. 52, no. 2, pp. 155–170, 1981.

[4] R. Agarwal and A. J. García, “Biomaterial strategies for engineering implants for enhanced osseointegration and bone repair,” *Adv. Drug Deliv. Rev.*, vol. 94, pp. 53–62, 2015.

[5] D. M. D. Ehrenfest, P. G. Coelho, B. Kang, Y. Sul, and T. Albrektsson, “Classification of osseointegrated implant surfaces : materials , chemistry and topography,” *Trends Biotechnol.*, vol. 28, no. 4, pp. 198–206, 2010.

[6] O. Hasturk, M. Ermis, U. Demirci, N. Hasirci, and V. Hasirci, “Square prism micropillars on poly(methyl methacrylate) surfaces modulate the morphology and differentiation of human dental pulp mesenchymal stem cells,” *Colloids Surfaces B Biointerfaces*, vol. 178, no. December 2018, pp. 44–55.

[7] C. Wang *et al.*, “Enhanced Osseointegration of Titanium Alloy Implants with Laser Microgrooved Surfaces and Graphene Oxide Coating,” *ACS Appl. Mater. Interfaces*, vol. 11, no. 43, pp. 39470–39483, 2019.

[8] Q. Ran *et al.*, “Osteogenesis of 3D printed porous Ti6Al4V implants with different pore sizes,” *J. Mech. Behav. Biomed. Mater.*, vol. 84, no. February, pp. 1–11, 2018.

[9] R. Staruch, M. Griffin, and P. Butler, “Nanoscale Surface Modifications of Orthopaedic Implants: State of the Art and Perspectives,” *Open Orthop. J.*, vol. 10, no. 1, pp. 920–938, 2017.

[10] I. Gnilitskyi *et al.*, “Cell and tissue response to nanotextured Ti6Al4V and Zr implants using high-speed femtosecond laser-induced periodic surface structures,” *Nanomedicine Nanotechnology, Biol. Med.*, vol. 21, p. 102036, 2019.

[11] G. Bissacco *et al.*, “Application of Functional Nano-Patterning to Polymer Medical Micro Implants,” pp. 474–477, 2015.

[12] P. T. Tang, J. D. Jensen, H. C. Dam, and P. Møller, “Microstructure & Other Properties of Pulse-Plated Copper for Electroforming Applications,” *Sur/Fin*, pp. 910–922, 2002.

[13] K. K. Saxena, M. Bellotti, J. Qian, and D. Reynaerts, “Characterization of Circumferential Surface Roughness of Micro-EDMed Holes Using Replica Technology,” *Procedia CIRP*, vol. 68, no. April, pp. 582–587, 2018.